

Article

Fabrication of PEO-PMMA-LiClO₄-Based Solid Polymer Electrolytes Containing Silica Aerogel Particles for All-Solid-State Lithium Batteries

Ye Sol Lim, Hyun-Ah Jung and Haejin Hwang *

Department of Materials Science and Engineering, Inha University, 100 Inha-ro, Michuhol-gu, Incheon 22212, Korea; yesol008@gmail.com (Y.S.L.); wjdgusdk824@gmail.com (H.-A.J.)

* Correspondence: hjhwang@inha.ac.kr; Tel.: +82-32-860-7521

Received: 3 September 2018; Accepted: 19 September 2018; Published: 26 September 2018



Abstract: To improve the ionic conductivity and thermal stability of a polyethylene oxide (PEO)-ethylene carbonate (EC)-LiClO₄-based solid polymer electrolyte for lithium-ion batteries, polymethyl methacrylate (PMMA) and silica aerogel were incorporated into the PEO matrix. The effects of the PEO:PMMA molar ratio and the amount of silica aerogel on the structure of the PEO-PMMA-LiClO₄ solid polymer electrolyte were studied by X-ray diffraction, Fourier-transform infrared spectroscopy and alternating current (AC) impedance measurements. The solid polymer electrolyte with PEO:PMMA = 8:1 and 8 wt% silica aerogel exhibited the highest lithium-ion conductivity ($1.35 \times 10^{-4} \text{ S}\cdot\text{cm}^{-1}$ at 30 °C) and good mechanical stability. The enhanced amorphous character and high degree of dissociation of the LiClO₄ salt were responsible for the high lithium-ion conductivity observed. Silica aerogels with a high specific surface area and mesoporosity could thus play an important role in the development of solid polymer electrolytes with improved structure and stability.

Keywords: solid polymer electrolyte; all-solid-state lithium battery; polyethylene oxide; conductivity; silica aerogel

1. Introduction

The constant development and widespread use of mobile devices are leading to increasing demand for secondary batteries for electrical energy storage. In particular, with the rapid growth in the smartphone market and the development of electric vehicles, the need for secondary batteries will continue to increase [1]. Current lithium-ion secondary batteries use a liquid electrolyte, whose leakage may cause fire and explosions, thus raising safety issues [2,3].

As a possible solution to this problem, all-solid-state lithium-ion batteries are being developed using a polymer or ceramic-based solid electrolyte [4,5]. The use of a solid electrolyte avoids risks of fire or explosions due to leakage and may also provide high capacity by reducing the cathodic limit of the potential window [6]. Among various solid electrolyte materials, solid polymers have been actively studied, owing to their good flexibility and interfacial stability [7].

Polyethylene oxide (PEO) presents various advantages, such as excellent interfacial stability with lithium, the formation of complexes with lithium salts, and a low glass transition temperature. However, the commercialization of PEO is difficult because its room-temperature ionic conductivity is as low as 10^{-7} – $10^{-6} \text{ S}\cdot\text{cm}^{-1}$ [8,9]. This is because the degree of crystallization of PEO increases at room temperature, whereas the mobility of lithium ions and thus the ionic conductivity are reduced [10]. In addition, the stability of PEO decreases at high temperatures, so that deformation easily occurs [11].

In order to reduce crystallinity and improve thermal stability, a PEO electrolyte was blended with TiO₂, SiO₂, and Al₂O₃ as inert inorganic fillers. Metal organic frameworks (MOF) with organic functional

groups are known to be an effective additive to improve lithium-ion conductivity and to control interfacial resistance between PEO-based solid electrolytes and electrodes [12,13]. Another method to improve the properties of the polymer electrolyte involves copolymerization with two or more polymers [14–16]. Recently, polymers including PEO have been prepared by a photo-induced polymerization technique which is a fast, environmentally benign and energy-efficient process [17–19].

In this study, PEO was copolymerized with polymethyl methacrylate (PMMA) to obtain a solid polymer electrolyte with improved ionic conductivity and thermal stability. In addition, silica aerogel particles were incorporated into the copolymerized PEO-PMMA electrolyte as inert inorganic fillers. Silica aerogel is a mesoporous material with extremely high porosity and a specific surface area. Further experiments were carried out to optimize the PEO:PMMA ratio and the silica aerogel content.

2. Materials and Methods

The polymer electrolyte was prepared from commercially available PEO (molecular weight, $M_w = 5,000,000$, Sigma-Aldrich, Gyeonggi, Korea) and PMMA ($M_w = 120,000$, Sigma-Aldrich, Gyeonggi, Korea). Acetonitrile (ACN, 99.8%, Samchun Pure Chemical, Pyeongtaek, Korea), LiClO_4 (99.99%, Sigma-Aldrich, Gyeonggi, Korea), and ethylene carbonate (EC, 98%, Sigma-Aldrich, Gyeonggi, Korea) were used as the solvents for lithium salt and plasticizer, respectively. A silica aerogel powder (Enova Aerogel IC3100) was purchased from Cabot Co.

PMMA was dissolved using ACN and the solution was stirred at 60 °C for 1 h. Then, PEO was added to the PMMA solution and mixed under the same conditions until a clear solution was obtained. EC and LiClO_4 were then added sequentially to the polymer solution and stirred at 60 °C for 12 h. Then, the silica aerogel powder was added to the polymer solution and stirred for another 24 h. Since EC and lithium salts are highly reactive with atmospheric moisture, the reaction was carried out in a glove box under a nitrogen atmosphere. The molar ratios of polymer to LiClO_4 and EC were 6:1 and 9:1, respectively. A total of 35.3 wt% of LiClO_4 was added to the polymers (PEO and PMMA). Finally, the polymer/lithium salt/silica aerogel mixture solution was poured into a mold and dried at 40 °C for 24 h under vacuum conditions, to obtain a thick film of solid electrolyte. Eleven (SP1 to SP6 and SP4-1 to SP4-5) solid polymer samples were prepared in this study and the PEO:PMMA ratios and silica aerogel content are shown in Table 1.

Table 1. Composition of the solid polymer electrolytes.

Sample Name	PEO:PMMA (Molar Ratio)	Silica Aerogel (wt%)
SP1	1:0	-
SP2	12:1	-
SP3	10:1	-
SP4	8:1	-
SP5	4:1	-
SP6	2:1	-
SP4-1	8:1	1
SP4-2	8:1	2
SP4-3	8:1	4
SP4-4	8:1	8
SP4-5	8:1	16

X-ray diffraction (XRD, DMAX 2200, Rigaku, Tokyo, Japan) measurements were performed to determine the degree of crystallinity of the solid polymer electrolyte. Thermal properties such as glass transition (T_g) and melting (T_m) temperatures were measured by differential scanning calorimetry (DSC, Perkin Elmer, Santa Clara, CA, USA). The DSC analysis was carried out at a heating rate of 10 °C·min⁻¹ under a nitrogen atmosphere, in the temperature range of −40 to 200 °C. The chemical structures of the polymer, lithium salt, and silica aerogel were analyzed by Fourier transform infrared spectroscopy (FT-IR, Vertex 80, Bruker, Ettlingen, Germany). The FT-IR measurements were performed

in the 600–3000 cm^{-1} range, at a resolution of 4 cm^{-1} . To measure the thermal stability of the polymer electrolyte samples, the film was placed and maintained for 6 h in a hot oven at 80 °C.

The lithium-ion conductivity of the solid electrolyte was analyzed by alternating current (AC) impedance spectroscopy (IM6e, Zahner, Kronach, Germany) measurements in a frequency range from 1 Hz to 1 MHz, at 30 °C. Pt blocking electrodes with a diameter of 10 mm were coated on both surfaces of the solid electrolyte and placed in contact with two aluminum disks.

3. Results and Discussion

The XRD patterns of various solid polymer electrolytes are shown in Figure 1. No peaks corresponding to crystalline PEO or PMMA are visible in the patterns of the SP1 to SP4 samples, consisting of PEO, LiClO_4 and EC, or PEO, PMMA, LiClO_4 , and EC. This indicates that the SP1, SP2, SP3, and SP4 samples are amorphous. In addition, no peaks corresponding to LiClO_4 could be identified in these four samples. This result suggests the complete dissolution of LiClO_4 in PEO or the blended polymer electrolytes with a PEO:PMMA ratio greater than eight [20].

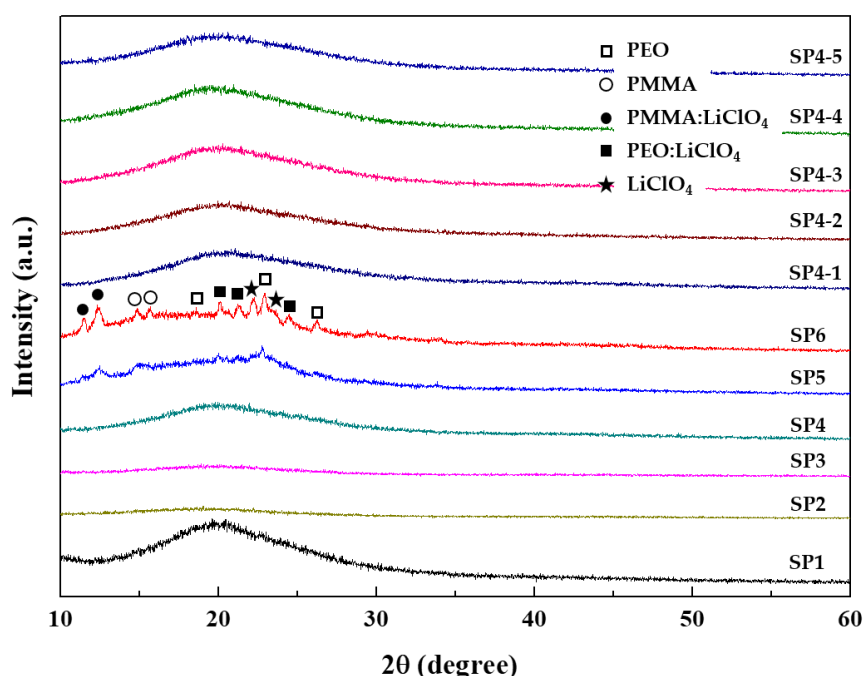


Figure 1. XRD patterns of solid polymer electrolyte samples.

Conversely, several sharp peaks associated with crystalline PEO, PMMA, PEO/ LiClO_4 , and PMMA/ LiClO_4 phases were observed in the SP5 and SP6 samples, confirming that the blend with a PEO:PMMA ratio of 4:1 lies at the boundary of the miscibility/immiscibility regions [21]. The relative intensities of all peaks corresponding to the crystalline phases increased with increasing PMMA molar amounts. The degree of crystallinity, thus, showed a strong dependence on the molar PEO:PMMA ratio. In the case of the SP5 and SP6 samples, the peaks observed at $2\theta = 22.5^\circ$ and 23.5° were assigned to the crystalline LiClO_4 phase [9,22]. In addition, their intensities increased with increasing PMMA molar amounts. Therefore, the incorporation of large amounts of PMMA appears to have had a negative impact on the LiClO_4 complexation with the polymer electrolyte.

Contrastingly, the addition of silica aerogel powder to the PEO-PMMA polymer did not have an effect on the miscibility or the degree of crystallinity. All solid polymer samples containing silica aerogel powder were found to be amorphous, with no visible XRD peaks associated with the crystalline phases or LiClO_4 . The complete dissolution of the Li salt in the polymer matrix was confirmed in the case of the SP1 to SP4 and SP4-1 to SP4-4 samples. This suggests that lithium-ion conduction

occurred in the amorphous region, so that the segmental motion of the PEO-PMMA matrix was further improved in the composite polymer electrolyte samples [23].

Figure 2a,b show the DSC and derivative curves, respectively, of the solid polymer electrolytes. No endothermic peak was observed in the SP1 to SP4 and SP4-1 to SP4-4 samples, whereas two endothermic peaks were found for the SP5 and SP6 samples. However, all solid polymer samples exhibited an exothermic peak at around -15 to -5 °C, which can be attributed to the glass transition of PEO- or PEO-PMMA-based solid polymer electrolytes.

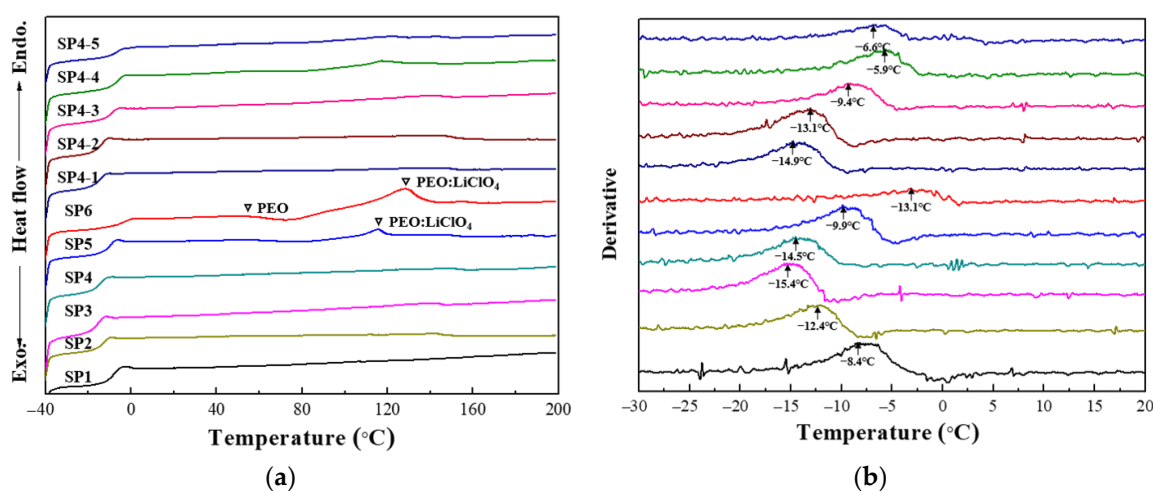


Figure 2. DSC (a) and derivative (b) curves of solid polymer electrolyte samples.

Based on the data in Figure 1, the absence of an endothermic peak (corresponding to the melting of crystalline PEO and PEO-PMMA) in the SP1 to SP4 and SP4-1 to SP4-4 samples was expected, because the PEO and PEO-PMMA samples complexed by LiClO_4 were amorphous [24,25]. In contrast, the endothermic peaks observed in SP5 and SP6 corresponded to the melting of crystalline phases such as PEO, PMMA and other complex phases.

In general, PEO and LiClO_4 formed several crystalline complexes, such as $(\text{PEO})_6:\text{LiClO}_4$ and $(\text{PEO})_3:\text{LiClO}_4$, depending on the PEO: LiClO_4 ratio, temperature and thermal history [26,27]. The melting temperature of the $(\text{PEO})_3:\text{LiClO}_4$ complex was 150 °C, while $(\text{PEO})_6:\text{LiClO}_4$ melts between 50 and 65 °C [21]. The endothermic peak at ~ 120 °C observed for SP5 and SP6 can be assigned to the crystalline $(\text{PEO})_3:\text{LiClO}_4$ phase, because the melting temperature of PEO was 44.04 °C and PMMA does not show endothermic peaks associated with melting in the temperature range from -40 to 200 °C [28]. The slightly lower melting temperature observed for SP5 and SP6 partially resulted from their high LiClO_4 :PEO ratio, because these samples were blended with PMMA.

The glass transition temperatures of the samples can be estimated from the derivatives of the DSC curves (Figure 2b). The T_g was found to be -8.4 °C for the PEO- LiClO_4 complex solid polymer, and gradually decreased with the increasing PEO:PMMA ratio for the PEO-PMMA- LiClO_4 solid polymer electrolytes. It is known that the T_g of PEO not complexed by LiClO_4 is -55 °C, and the T_g value increases with increasing LiClO_4 molar amounts [29]. The T_g measured for SP1 was in good agreement with the results obtained by Fullerton et al. [24]. However, the T_g of the solid polymer electrolytes containing silica aerogel powder was higher than that of the silica aerogel-free samples. Inert ceramic fillers such as silica aerogel can alter the crystallinity or the stiffness of polymer chains, resulting in an increase in the T_g of solid polymer electrolytes [30,31].

Figure 3 shows the FT-IR spectra of the solid polymer electrolyte samples. The peak at 1100 cm^{-1} can be assigned to the C-O-C stretching of ether links in PEO. In addition, a peak attributed to the C-H stretching of PEO was observed near 2900 cm^{-1} , and its intensity decreased with increasing PMMA molar amounts. The peaks observed at 625 and 939 cm^{-1} were assigned to ClO_4^- [32], while a peak

corresponding to uncomplexed LiClO_4 was observed at 1640 cm^{-1} in all solid polymer electrolyte samples [33].

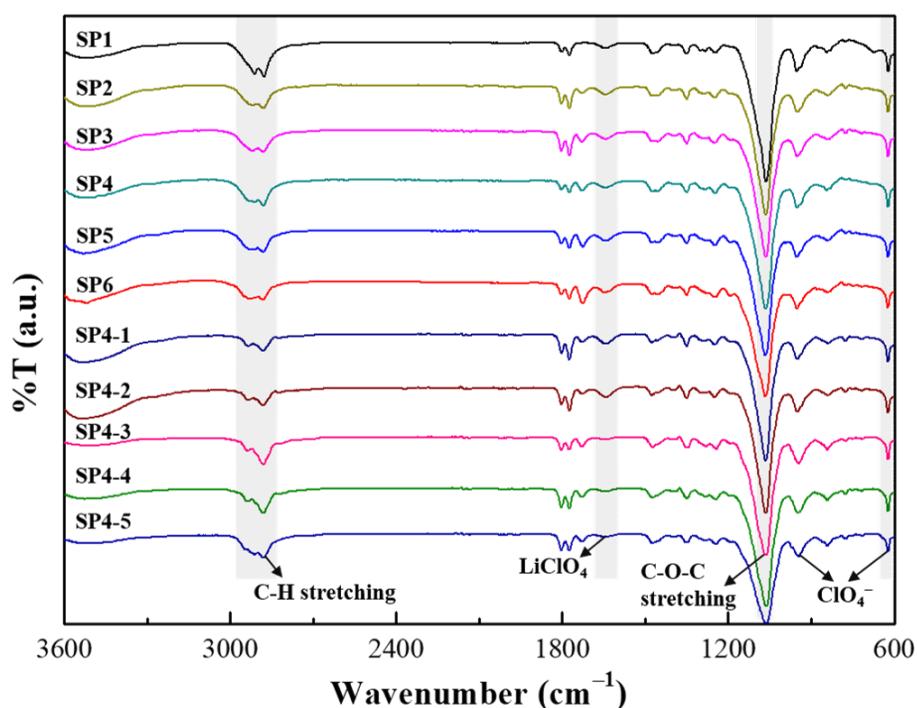


Figure 3. FT-IR spectra of solid polymer electrolyte samples.

The intensity of the peak corresponding to LiClO_4 was slightly higher in the SP5 and SP6 than the SP1 to SP4 samples. This is in good agreement with the XRD results in Figure 1. In contrast, the intensity of the free ClO_4^- peak at 625 cm^{-1} increased as the PEO:PMMA molar ratio decreased to eight; however, the ClO_4^- peak intensity decreased with increasing PMMA molar content. These results suggest that PMMA blending with the PEO matrix favors the dissociation of LiClO_4 and the formation of PEO- LiClO_4 complexes. However, when the PEO to PMMA molar ratio decreased to four and three, phase separation between PEO and PMMA occurred, which resulted in a decrease in the degree of dissociation of the lithium salt.

An interesting feature observed in Figure 3 is that the addition of silica aerogel to the PEO-PMMA polymer electrolyte favored the dissociation of LiClO_4 and its complexation with the polymer matrix. As a result, the intensity of the peak corresponding to LiClO_4 decreased in the SP4-1 to SP4-4 samples, whereas the intensity of the free ClO_4^- peak at 600 cm^{-1} increased.

Figure 4 shows the AC impedance spectra of symmetrical cells consisting of a solid polymer electrolyte and two Pt blocking electrodes, measured at $30\text{ }^\circ\text{C}$, along with their equivalent circuit model. The spectra show a semicircle at high frequency followed by a spike at low frequency, often observed in symmetrical cells with blocking electrodes. The equivalent circuit is composed of R_b and C_b in parallel, connected in series with C_e , where R_b and C_b are the bulk resistance and capacitance of the electrolyte, respectively, and C_e is the interfacial capacitance. Among these circuit elements, the bulk resistance of the solid polymer electrolyte corresponds to the diameter of the semicircle in the Nyquist plot shown in Figure 4. The lithium-ion conductivity can be calculated from the bulk resistance, the thickness of the electrolyte, and the area of the electrode. Table 2 shows the lithium-ion conductivity of the solid polymer electrolyte samples.

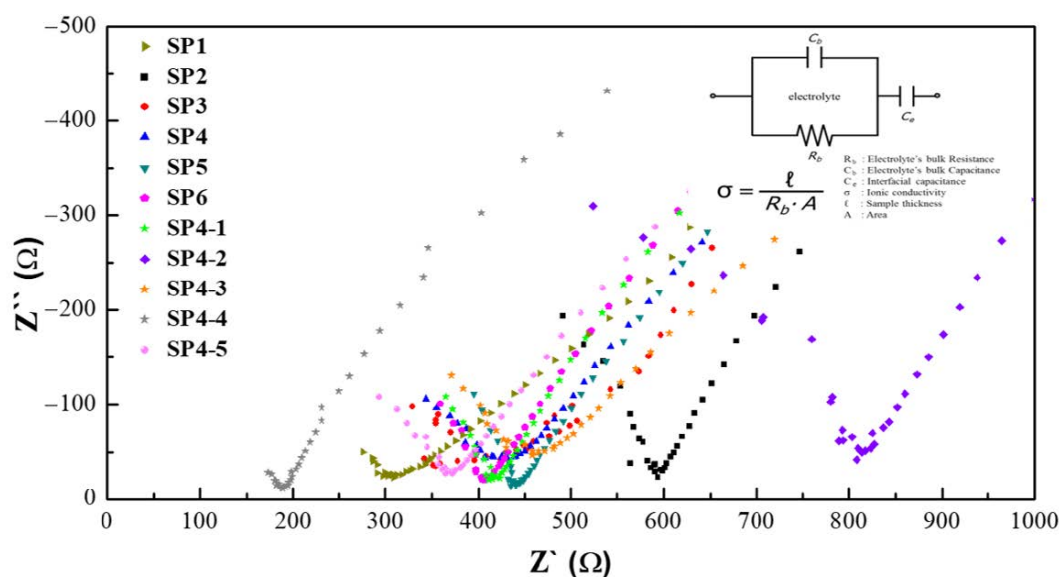


Figure 4. AC impedance spectra of solid polymer electrolyte samples.

Table 2. Lithium-ion conductivities of solid polymer electrolyte samples.

Sample	PEO:PMMA (Molar Ratio)	Silica Aerogel (wt%)	Ion Conductivity ($\text{S}\cdot\text{cm}^{-1}$, at 30 °C)
SP1	1:0	-	2.36×10^{-5}
SP2	12:1	-	3.64×10^{-5}
SP3	10:1	-	6.18×10^{-5}
SP4	8:1	-	6.70×10^{-5}
SP5	4:1	-	4.63×10^{-5}
SP6	2:1	-	4.40×10^{-5}
SP4-1	8:1	1	2.52×10^{-5}
SP4-2	8:1	2	2.83×10^{-5}
SP4-3	8:1	4	5.37×10^{-5}
SP4-4	8:1	8	1.35×10^{-4}
SP4-5	8:1	16	1.02×10^{-4}

Figure 5a shows the lithium-ion conductivities of the solid polymer electrolyte samples as a function of the PMMA molar ratio. The Li-ion conductivity increases with increasing PMMA molar amounts. The highest conductivity was obtained for the solid polymer electrolyte sample with PEO:PMMA = 8:1. The ion conductivity of PEO depends on the degree of crystallinity and the solubility of the lithium salt. Blending PMMA with PEO can result in a PEO-PMMA polymer with low degree of crystallinity, along with a low glass transition temperature. As was shown in Figure 2, the T_g of the PEO-PMMA blended polymer decreased with the addition of PMMA [34,35]. However, the further addition of PMMA led to a gradual decrease in conductivity. This phenomenon can be explained by the immiscibility between PEO and PMMA in solid polymer samples with high PMMA molar amounts, as shown in Figure 1. The formation of crystalline PEO- and PMMA-based polymers resulted in a severe decrease in carrier (i.e., lithium-ion) mobility.

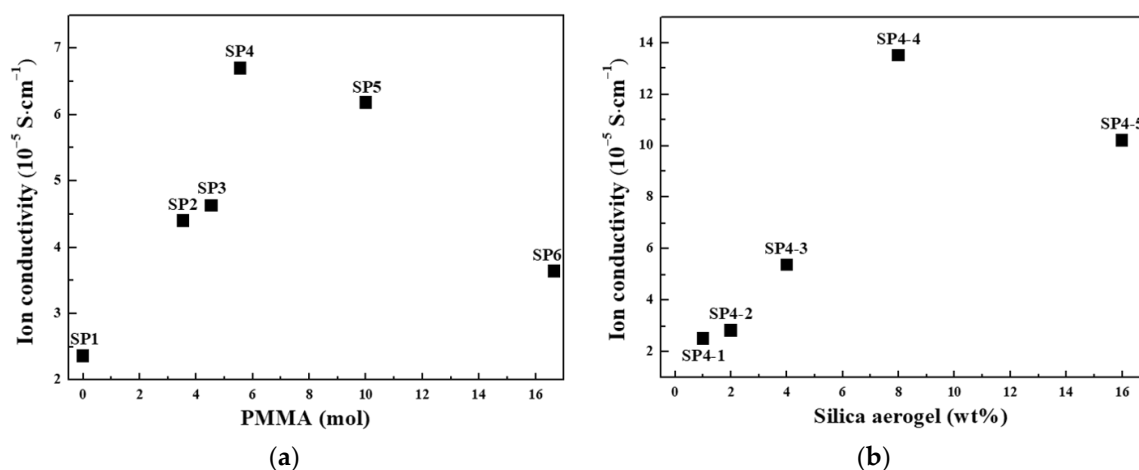


Figure 5. Lithium-ion conductivity of solid polymer electrolyte samples as a function of PMMA (a) and silica aerogel (b) content.

The addition of silica aerogel powder to the PEO-PMMA blended polymer matrix effectively enhanced its conductivity. As the silica aerogel content was increased, the conductivity first increased, reaching a maximum at 8 wt%, and then decreased upon the further addition of silica aerogel. The highest conductivity of $1.35 \times 10^{-4} \text{ S}\cdot\text{cm}^{-1}$ was achieved for the SP4-3 sample. The incorporation of nanosized ceramic fillers such as TiO_2 , SiO_2 , ZrO_2 , and Al_2O_3 has been extensively used to enhance the lithium-ion conductivity of PEO and its related polymer electrolytes, as first proposed by Wieczorek et al. [36].

Ceramic fillers, and especially TiO_2 nanoparticles, provide Lewis acid centers that can induce Lewis acid-based interactions between the polar surface of ceramic particles and lithium ions, which in turn create highly conducting transient pathways for lithium ions in the polymer electrolyte [37–39]. Although the strength of the Lewis acid center of SiO_2 is much lower than that of TiO_2 , the Lewis acid-based interactions may be enhanced in the solid polymer electrolyte samples containing silica aerogel due to the extremely large specific surface area of the silica aerogel powder used in this study. In addition, the silica aerogel promotes Li salt dissociation, because the Lewis acid-base interactions between silica aerogel and lithium ions weaken the $\text{Li}^+\text{-ClO}_4^-$ ionic couple [40]. As is shown in Figure 3, the FT-IR intensity of the ClO_4^- peak increased with the increasing silica aerogel content. The increase in conductivity of the polymer electrolyte samples containing silica aerogel powder could be ascribed to the enhanced dissociation of the Li salt promoted by the silica aerogel.

The SP4-1, SP4-2, and SP4-3 samples exhibited lower conductivity than SP4. This was attributed to the fact that the high degree of dissociation induced by the silica aerogel was counteracted by the volumetric effect. When the silica aerogel content exceeded 8 wt%, e.g., in the SP4-5 sample, it was difficult to obtain a homogeneous film without cracks or defects.

Solid polymers used as electrolytes for lithium-ion secondary batteries are required to withstand unexpected temperature increases. Therefore, it is extremely important to develop solid polymer electrolytes with high stability at elevated temperatures. The thermal and mechanical stabilities of the solid polymer electrolyte samples are displayed in Figure 6. The polymer samples were heat-treated at 80°C for 6 h and subsequently folded or stretched. The SP1 sample, consisting of PEO and LiClO_4 , exhibited poor thermal and mechanical stability compared to samples blended with PMMA or silica aerogel powder. In particular, Figure 6b,c show that the SP1 sample did not recover its original film shape after being folded, and tore upon stretching.

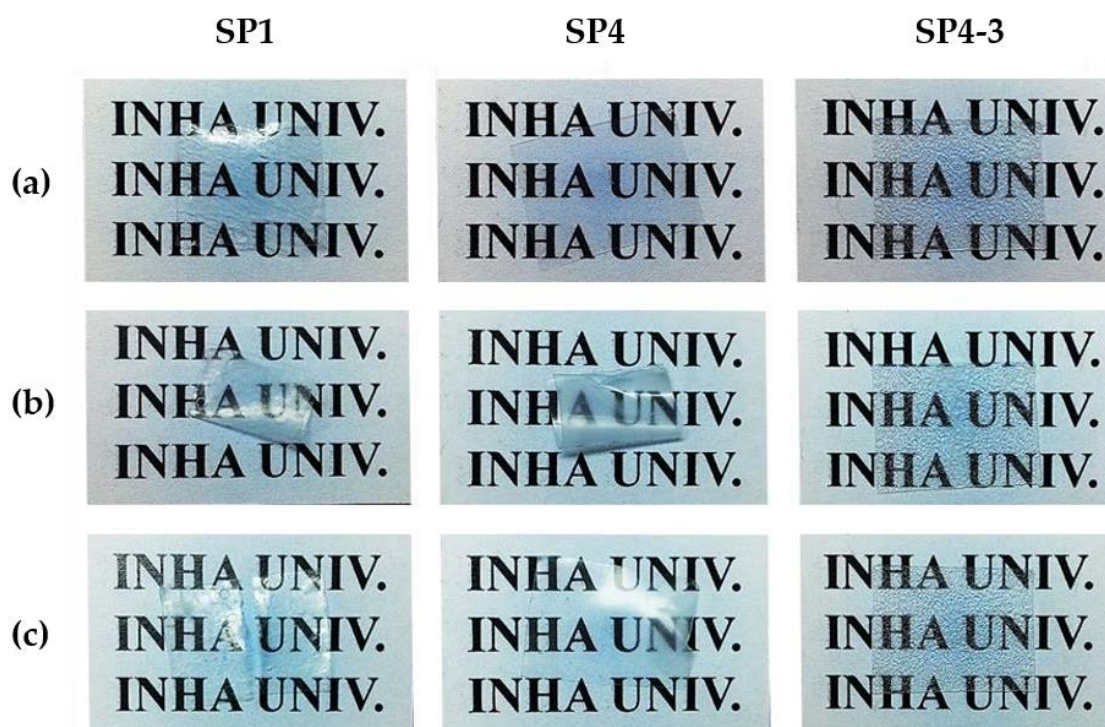


Figure 6. Photographs of (a) As-prepared solid polymer electrolyte samples, (b) Solid polymer samples which were heat-treated at 80 °C for 6 h and then folded, and (c) Solid polymer samples which were heat-treated at 80 °C for 6 h and then stretched.

In contrast, the SP4 and SP4-3 samples exhibited superior thermal and mechanical properties to SP1, which suggests that PMMA blending and incorporation of silica aerogel powder effectively allows the acquisition of thermally and mechanically stable solid electrolytes [41]. In particular, the SP4-3 sample, containing 8 wt% silica aerogel and possessing the highest lithium-ion conductivity, showed no shrinkage or shape change after the application of thermal and mechanical stresses.

4. Conclusions

We fabricated PEO-PMMA-EC-LiClO₄-based solid polymer electrolytes containing silica aerogel particles and investigated the dependence of their structure, thermal behavior, and lithium-ion conductivity on the PEO:PMMA ratio and silica aerogel content. The XRD and FT-IR analyses show that blending PMMA with PEO effectively retards the crystallization of the polymers and reduces their glass transition temperature, which in turn leads to enhanced lithium-ion conductivity. The solid polymer sample with PEO:PMMA = 8:1 (SP4) exhibited good conductivity ($6.90 \times 10^{-5} \text{ S}\cdot\text{cm}^{-1}$). The ionic conductivity of the blended PEO-PMMA-EC-LiClO₄ solid polymer electrolyte was further increased by incorporating silica aerogel powder. The conductivity increased with the silica aerogel content, which might be due to the higher degree of lithium salt dissociation. The sample incorporating 8 wt% silica aerogel showed the highest conductivity, with a value of $1.35 \times 10^{-4} \text{ S}\cdot\text{cm}^{-1}$. However, the incorporation of 16 wt% silica aerogel did not result in a further increase in conductivity. This effect is due to the aggregation of silica aerogel, which reduces the mobility of lithium ions. Finally, the addition of PMMA and silica aerogel significantly improved the thermal and mechanical stabilities of the PEO-based solid polymer electrolyte.

Author Contributions: Conceptualization, H.H.; investigation, H.-A.J.; supervision, H.H.; and writing—original draft, Y.S.L.

Funding: This work was supported by the National Research Foundation of Korea (NRF) grant funded by the Korea government (MSIT) (No. 2016R1A2B2011517). This work was supported by the Korea Institute of Energy

Technology Evaluation and Planning (KETEP) and the Ministry of Trade, Industry & Energy (MOTIE) of the Republic of Korea (No. 20174030201500).

Conflicts of Interest: The authors declare no conflicts of interest.

References

1. Gao, R.; Nam, H.O.; Ko, W.I.; Jang, H. National Options for a Sustainable Nuclear Energy System: MCDM Evaluation Using an Improved Integrated Weighting Approach. *Energies* **2017**, *10*, 2017. [[CrossRef](#)]
2. Kang, Y.K.; Lee, C.J. Polymer electrolytes for lithium polymer batteries. *Polym. Sci. Technol.* **2003**, *14*, 396–406.
3. Kermani, G.; Sahraei, E. Review: Characterization and Modeling of the Mechanical Properties of Lithium-Ion Batteries. *Energies* **2017**, *10*, 1730. [[CrossRef](#)]
4. Park, M.; Jung, W.D.; Choi, S.; Son, K.; Jung, H.; Kim, B.; Lee, H.; Lee, J.; Kim, H. Microscopic analysis of high lithium-ion conducting glass-ceramic sulfides. *J. Korean Ceram. Soc.* **2016**, *53*, 568–573. [[CrossRef](#)]
5. Shin, R.H.; Son, S.I.; Lee, S.M.; Han, Y.S.; Kim, Y.D.; Ryu, S.S. Effect of Li_3BO_3 additive on densification and ion conductivity of garnet-type $\text{Li}_7\text{La}_3\text{Zr}_2\text{O}_{12}$ solid electrolytes of all-solid-state lithium-ion batteries. *J. Korean Ceram. Soc.* **2016**, *53*, 712–718. [[CrossRef](#)]
6. Quartarone, E.; Mustarelli, P. Electrolytes for solid-state lithium rechargeable batteries: Recent advances and perspectives. *Chem. Soc. Rev.* **2011**, *40*, 2525–2540. [[CrossRef](#)] [[PubMed](#)]
7. Fergus, J.W. Ceramic and polymeric solid electrolytes for lithium-ion batteries. *J. Power Sources* **2010**, *195*, 4554–4569. [[CrossRef](#)]
8. Liang, G.; Xu, J.; Xu, W.; Shen, X.; Zhang, H.; Yao, M. Effect of filler-polymer interactions on the crystalline morphology of PEO-based solid polymer electrolytes by Y_2O_3 nano-fillers. *Polym. Compos.* **2011**, *32*, 511–518. [[CrossRef](#)]
9. Jung, Y.C.; Park, M.S.; Doh, C.H.; Kim, D.W. Organic-inorganic hybrid solid electrolytes for solid-state lithium cells operating at room temperature. *Electrochim. Acta* **2016**, *218*, 271–277. [[CrossRef](#)]
10. Benedicta, T.J.; Banumathia, S.; Veluchamy, A.; Gangadharana, R.; Ahamadb, A.Z.; Rajendranb, S. Characterization of plasticized solid polymer electrolyte by XRD and AC impedance methods. *J. Power Sources* **1998**, *75*, 171–174. [[CrossRef](#)]
11. Michael, M.S.; Jacob, M.M.E.; Prabakaran, S.R.S.; Radhakrishna, S. Enhanced lithium ion transport in PEO-based solid polymer electrolytes employing a novel class of plasticizers. *Solid State Ion.* **1997**, *98*, 167–174. [[CrossRef](#)]
12. Suriyakumar, S.; Gopi, S.; Kathiresan, M.; Bose, S.; Gowd, E.B.; Nair, J.R.; Angulakshmi, N.; Meligrana, G.; Bella, F.; Gerbaldi, C.; et al. Metal organic framework laden poly (ethylene oxide) based composite electrolytes for all-solid-state Li-S and Li-metal polymer batteries. *Electrochim. Acta* **2018**, *285*, 355–364. [[CrossRef](#)]
13. Xu, G.; Nie, P.; Dou, H.; Ding, B.; Li, L.; Zhang, X. Exploring metal organic frameworks for energy storage in batteries and supercapacitors. *Mater. Today* **2017**, *20*, 191–209. [[CrossRef](#)]
14. Yoon, M.Y.; Hong, S.K.; Hwang, H.J. Fabrication of Li-polymer/silica aerogel nanocomposite electrolyte for an all-solid-state lithium battery. *Ceram. Int.* **2013**, *39*, 9659–9663. [[CrossRef](#)]
15. Lee, L.G.; Park, S.J.; Kim, S. Study on ionic conductivity and crystallinity of PEO/PMMA polymer composite electrolytes containing TiO_2 filler. *Korean Chem. Eng. Res.* **2011**, *49*, 758–763. [[CrossRef](#)]
16. Liang, B.; Tang, S.; Jiang, Q.; Chen, C.; Chen, X.; Li, S.; Yan, X. Preparation and characterization of PEO-PMMA polymer composite electrolytes doped with nano- Al_2O_3 . *Electrochim. Acta* **2015**, *169*, 334–341. [[CrossRef](#)]
17. Radzir, N.N.M.; Hanifah, S.A.; Ahmad, A.; Hassan, N.H.; Bella, F. Effect of lithium bis(trifluoromethylsulfonyl)imide salt-doped UV-cured glycidyl methacrylate. *J. Solid State Electrochem.* **2015**, *19*, 3079–3085. [[CrossRef](#)]
18. Colò, F.; Bella, F.; Nair, J.R.; Gerbaldi, C. Light-cured polymer electrolytes for safe, low-cost and sustainable sodium-ion batteries. *J. Power Sources* **2017**, *365*, 293–302. [[CrossRef](#)]
19. Bella, F.; Colò, F.; Nair, J.R.; Gerbaldi, C. Photopolymer Electrolytes for Sustainable, Upscalable, Safe, and Ambient-Temperature Sodium-Ion Secondary Batteries. *ChemSusChem* **2015**, *8*, 3668–3676. [[CrossRef](#)] [[PubMed](#)]
20. Rajendran, S.; Sivakumar, M.; Subadevi, R. Investigations on the effect of various plasticizers in PVA-PMMA solid polymer blend electrolytes. *Mater. Lett.* **2004**, *58*, 641–649. [[CrossRef](#)]

21. Dionísio, M.; Fernandes, A.C.; Mano, J.F.; Correia, N.T.; Sousa, R.C. Relaxation studies in PEO/PMMA blends. *Macromolecules* **2000**, *33*, 1002–1011. [[CrossRef](#)]
22. Flora, X.H.; Ulaganathan, M.; Rajendran, S. Influence of lithium salt concentration on PAN-PMMA blend polymer electrolytes. *Int. J. Electrochem. Sci.* **2012**, *7*, 7451–7462.
23. Meyer, W.H. Polymer electrolytes for lithium-ion batteries. *Adv. Mater.* **1998**, *10*, 439–448. [[CrossRef](#)]
24. Fullerton-Shirey, S.K.; Maranas, J.K. Effect of LiClO₄ on the structure and mobility of PEO-based solid polymer electrolytes. *Macromolecules*. **2009**, *42*, 2142–2156. [[CrossRef](#)]
25. Wang, Y.J.; Pan, Y.; Wang, L.; Pang, M.J.; Chen, L. Characterization of (PEO)LiClO₄-Li_{1.3}Al_{0.3}Ti_{1.7}(PO₄)₃ composite polymer electrolytes with different molecular weights of PEO. *J. Appl. Polym. Sci.* **2006**, *102*, 4269–4275. [[CrossRef](#)]
26. Robitaille, C.D.; Fauteux, D. Phase diagrams and conductivity characterization of some PEO-LiX electrolytes. *J. Electrochem. Soc.* **1986**, *133*, 315–325. [[CrossRef](#)]
27. Fullerton-Shirey, S.K.; Maranas, J.K. Structure and mobility of PEO/LiClO₄ solid polymer electrolytes filled with Al₂O₃ nanoparticles. *J. Phys. Chem. C* **2010**, *114*, 9196–9206. [[CrossRef](#)]
28. Kumar, M.; Chung, J.S.; Hur, S.H. Controlled atom transfer radical polymerization of MMA onto the surface of high-density functionalized graphene oxide. *Nanoscale Res. Lett* **2014**, *9*, 345–351. [[CrossRef](#)] [[PubMed](#)]
29. Munichandraiah, N.; Scanlon, L.G.; Marsh, R.A.; Kumar, B.; Sircar, A.K. Influence of zeolite on electrochemical and physicochemical properties of polyethylene oxide solid electrolyte. *J. Appl. Electrochem.* **1995**, *25*, 857–863. [[CrossRef](#)]
30. Kim, Y.W.; Lee, W.; Choi, B.K. Relation between glass transition and melting of PEO–salt complexes. *Electrochim. Acta* **2000**, *45*, 1473–1477. [[CrossRef](#)]
31. Kweon, J.-O.; Noh, S.-T. Thermal, thermomechanical, and electrochemical characterization of the organic–inorganic hybrids poly(ethylene oxide) (PEO)–silica and PEO–silica–LiClO₄. *J. Appl. Polym. Sci.* **2001**, *81*, 2471–2479. [[CrossRef](#)]
32. Licoccia, S.; Trombetta, M.; Capitani, D.; Proietti, N.; Romagnoli, P.; Vona, M.L.D. ATR–FTIR and NMR spectroscopic studies on the structure of polymeric gel electrolytes for biomedical applications. *Polymer* **2005**, *46*, 4670–4675. [[CrossRef](#)]
33. Shukla, N.; Thakur, A.K. Role of salt concentration on conductivity optimization and structural phase separation in a solid polymer electrolyte based on PMMA–LiClO₄. *Ionics* **2009**, *15*, 357–367. [[CrossRef](#)]
34. Song, J.Y.; Wang, Y.Y.; Wan, C.C. Review of gel-type polymer electrolytes for lithium-ion batteries. *J. Power Sources* **1999**, *77*, 183–197. [[CrossRef](#)]
35. Hu, H.; Yuan, W.; Lu, L.; Zhao, H.; Jia, Z.; Baker, G.L. Low glass transition temperature polymer electrolyte prepared from ionic liquid grafted polyethylene oxide. *J. Polym. Sci. Part A Polym. Chem.* **2014**, *52*, 2104–2110. [[CrossRef](#)]
36. Wiczorek, W.; Florjanczyk, Z.; Stevens, J.R. Composite polyether based solid electrolytes. *Electrochim. Acta* **1995**, *40*, 2251–2258. [[CrossRef](#)]
37. Croce, F.; Persi, L.; Scrosati, B.; Serraino-Fiory, F.; Plichta, E.; Hendrickson, M.A. Role of the ceramic fillers in enhancing the transport properties of composite polymer electrolytes. *Electrochim. Acta* **2011**, *46*, 2457–2461. [[CrossRef](#)]
38. Jayathilaka, P.A.R.D.; Dissanayake, M.A.K.L.; Albinsson, I.; Mellander, B.-E. Effect of nano-porous Al₂O₃ on thermal, dielectric and transport properties of the (PEO)₉LiTFSI polymer electrolyte system. *Electrochim. Acta* **2002**, *47*, 3257–3268. [[CrossRef](#)]
39. Panero, S.; Scrosati, B.; Sumathipala, H.H.; Wiczorek, W. Dual-composite polymer electrolytes with enhanced transport properties. *J. Power Sources* **2007**, *167*, 510–514. [[CrossRef](#)]
40. Vignarooban, K.; Dissanayake, M.A.K.L.; Albinsson, I.; Mellander, B.-E. Effect of TiO₂ nano-filler and EC plasticizer on electrical and thermal properties of poly (ethylene oxide) (PEO) based solid polymer electrolytes. *Solid State Ion.* **2014**, *266*, 25–28. [[CrossRef](#)]
41. Parale, V.G.; Lee, K.-Y.; Park, H.-H. Flexible and transparent silica aerogels: An overview. *J. Korean Ceram. Soc.* **2017**, *54*, 184–199. [[CrossRef](#)]

